Spectroscopic Signatures of VOC Physisorption on Microporous Solids. Application for Trichloroethylene and Tetrachloroethylene Adsorption on MFI Zeolites

O. Bertrand,* G. Weber, S. Maure, V. Bernardet, J. P. Bellat, and C. Paulin

Laboratoire de Recherches sur la Réactivité des Solides, UMR 5613, 9, avenue Alain Savary − B. P. 47870-21078 DIJON Cedex, France

Received: April 8, 2004; In Final Form: May 2, 2005

This paper presents an experimental infrared spectroscopic study of the physisorption of trichloroethylene (TCE) and tetrachloroethylene (PCE) on a self-supported high silica ZSM5 zeolite. The evolution of the shape, area, and location of vibration bands of both the adsorbent and the adsorbate is analyzed with respect to the number of sorbed molecules. The state of the adsorbed phase is characterized upon adsorption by comparing the location of the investigated vibration bands with the location of the corresponding vibration bands of the chloroalkenes in gaseous, liquid, and solid phases. The singular behavior of PCE with respect to TCE is seen from the modification of vibration bands of both the adsorbed phase and the adsorbent upon loading. The adsorption process proceeds by stages for PCE, whereas it appears continuous for TCE. Particular micropore loadings are evidenced at 4 and 6.5 molec.uc^{-1} for PCE and at 6 molec.uc^{-1} for TCE, in agreement with previous macroscopic and microscopic data. In addition, the presence of admolecules induces at least one emerging vibration band located at around 1715 cm^{-1}, mainly due to a contribution of the microporous surface of the adsorbent.

1. Introduction

Volatile organic compounds (VOCs) are the byproducts of many industrial processes. These compounds are causing concerns due to the dangers they pose to human health and to the destruction of the ozone layer in the stratosphere.[1,2] Catalytic oxidation, thermal incineration, biological treatments, or regenerative thermal treatments are destruction methods currently used to control VOC emission.[3−6] Another interesting alternative consists of recovering the organic substances by adsorption processes. For recovery methods, organic compounds are separated from the polluted effluent, then concentrated and recycled in the industrial process. Activated carbons are often used as industrial adsorbents because of their high adsorption capacity and their interesting cost in use. In counterpart, they have disadvantages in that they are hydrophilic, inflammable, and incompletely regenerable, which hydrophobic zeolites do not show.

The choice of the adsorbent mainly lies in two considerations. At first, it must have pores larger than the largest molecules to be adsorbed. This criterion is stricter for zeolites than for activated carbons or polymers because zeolites show uniform and narrower pore size distribution. Moreover, the adsorbent must exhibit a high enough adsorption affinity of the compounds but up to a certain extent to be regenerated at low temperature. One way to optimize the choice of an adsorbent for an industrial application is to characterize pure gas adsorption equilibria, then to determine physicochemical mechanisms during the adsorption process.

Physisorption of organic compounds on MFI zeolites usually gives rise to classical type I isotherms. However, stepped isotherms may be sometimes observed, as for the adsorption of some aromatic compounds (benzene, toluene, ethylbenzene, *p*-xylene, bromobenzene...)[7−16] or some linear paraffinic hydrocarbons (*n*-hexane, *n*-heptane).[17,18] The origin of stepped isotherms was largely discussed in the literature.[19−23] For most authors, it is related to a phase transition of the adsorbate and/or the adsorbent.

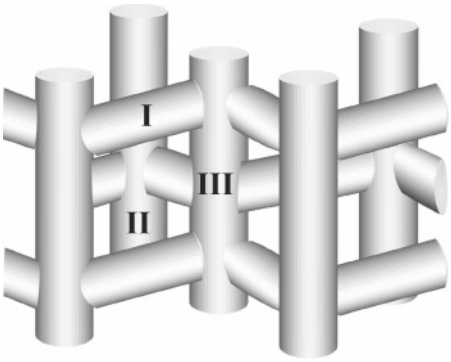

Figure 1. Shematic representation of the microporous network of MFI zeolites, which consists of interconnected straight and sinusoidal channels (sites I, sinusoidal channels; sites II, straight channels; sites III, intersections of straight and sinusoidal channels).

Concerning chloroalkene derivatives, we have more particularly studied the interaction of tetrachloroethylene (PCE) and trichloroethylene (TCE) on high silica MFI zeolites using thermogravimetry, microcalorimetry, in situ X-ray diffraction, and in situ neutron diffraction. These chlorinated solvents of molecular size close to the pore opening of the zeolite of around 0.6 nm[24,25] do not interact in the same way with MFI zeolites (Figure 1). Indeed, sorption isotherms for TCE are of type I at 298 K, whereas those for PCE display a step at half loading (4 molec.uc^{-1}) and at very low relative pressure ($p/p_0 = 0.02$).[26−29] Moreover, the adsorption capacity of MFI zeolites for these VOCs is higher for TCE than for PCE. The singular character of PCE was also underlined by the discontinuous shape of

* Corresponding author. E-mail: odile.bertrand@u-bourgogne.fr.

10.1021/jp048442a CCC: $30.25
Published on Web 06/18/2005

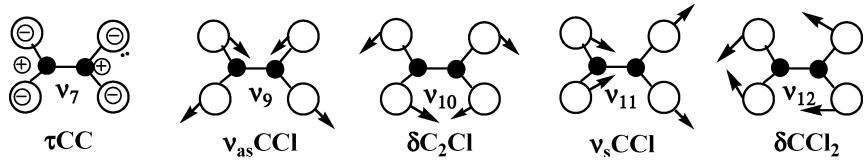

Figure 2. Infrared active fundamental vibrations[46] of the tetrachloroethylene molecule. Plus (+) and minus (−) signs are used to represent a torsion movement ahead and behind of the plane of the molecule (●, C; ○, Cl).

enthalpy and entropy curves.[9,26−29] Heat curves show a stepwise increase of around 10 kJ.mol^{-1} followed by a plateau region at the step in the isotherms. Entropy curves exhibit a steep decrease in the range 2.5−4 molec.uc^{-1} above which a plateau region was also observed at the step in the isotherms. For comparison, the heat and entropy curves for TCE adsorption display a classical shape typical of microporous adsorbents. On the other hand, structural data characterized a high flexibility of the framework of high silica MFI zeolites. A monoclinic-orthorhombic structural change was observed at 4 and 6 molec.uc^{-1} for the adsorption of PCE and TCE, respectively.[28−34] Neutron diffraction data[30] indicated that adsorbates undergo no phase transition and that micropore filling proceeds by sites. For TCE, molecules indifferently fill all parts of microporosity. For PCE, a two-stage process of micropore filling was characterized: up to 4 molec.uc^{-1}, admolecules fill only intersections (sites III), and after, indifferently straight (sites II) and sinusoidal (sites I) channels (Figure 1).

In the present paper, we report another study of the interaction of PCE and TCE on a high silica ZSM-5 zeolite, by means of in situ FTIR spectroscopy.[35] This technique is largely used to characterize the surface acidity of zeolite catalysts (Lewis and Brönsted acidities) by means of suitable molecular probes.[36,37] In counterpart, infrared spectroscopic studies dedicated to pure physisorption phenomena on zeolites are scarce. In most cases, the spectra of adsorbed molecules are analyzed upon adsorption either to estimate the electric field in adsorption sites[38−40] or to characterize the binding state and the conformation of adsorbed molecules.[41−43] In a few cases, the evolution of the zeolite spectrum is also studied but mainly in the hydroxyl vibration region.[44] So far as we know, no studies are performed to characterize the modification of zeolite framework vibration bands on loading.

The first part of the paper is dedicated to the experimental study of the infrared spectra of PCE and TCE in gaseous, liquid, and solid phases to further characterize the state of the adsorbed phases during the adsorption process. The second part reports the change of the infrared spectrum of the adsorbent upon loading. Spectroscopic data are correlated to previous experimental results obtained by other macroscopic and microscopic techniques.

2. Experimental Section

Zeolite and Chloroalkenes. The template-powder parent Na-ZSM-5 zeolite (Si/Al = 500) was supplied by DEGUSSA. Prior to adsorption experiments, the TPA (tetrapropylammonium) template was removed by calcination under air at 873 K for 24 h to release the microporosity of the zeolite. This adsorbent does not show as the H-form of MFI zeolites of low Si/Al ratio, any catalytic behavior for the oxidative destruction of single and binary mixtures of chlorinated VOC compounds at room temperature.[5,6]

Self-supported wafers were compressed under a uniaxial pressure of 0.20 GPa to not significantly change the physical properties of the zeolite (crystallinity, adsorption properties...).[28] Only pieces of wafers were prepared under these conditions because a low weight of sample (2 mg) was used to allow an analysis by IR transmission. The use of a constant weight of sample ensured the preparation of wafers with the same thickness. Some physicochemical characteristics of the powder template-free sample were reported elsewhere.[28] The chemicals PCE and TCE distributed by PROLABO (R. P. Products) were of purity greater than 99% and contain a water amount of around 0.0050%. For adsorption experiments, they were stored in an evacuated vessel containing a 3A hydrophilic zeolite to trap any residual water.

Sample Preparation for FTIR Analysis of Pure Chloroalkenes. Samples were analyzed in a standard Cole Palmer cell consisting of two KBr windows with a spacer of between 2 mm and 100 μm for gaseous and liquid chloroalkenes, respectively. KBr windows were changed after each analysis to provide good quality spectra. Chloroalkenes in solid state were prepared at low temperature, by dispersing a drop of liquid on the surface of a very thin filter paper cooled at 77 K, and then immediately analyzed. FTIR spectra of chloroalkenes were collected in a 1725X Perkin-Elmer spectrometer by co-adding 100 scans in the wavenumber range 4000−400 cm^{-1}. The resolution of the spectrophotometer was 4 cm^{-1}.

In Situ FTIR Spectroscopy for Studying Adsorption Processes at Room Temperature. The spectroscopic study was performed using an original home-built glass system[35] to prevent adsorption of gases on the walls of the experimental setup. The upper part of the experimental setup allows in situ heat treatments up to 673 K in high vacuum (10^{-2} Pa). The optical cell sealed with two KBr windows is located in the lower part of the system. A suitable IR home-built sample holder containing zeolite wafer pieces can be moved up and down by means of a magnetization system. The cell is connected on one hand to a vacuum system and on the other hand to the gaseous adsorptive. A Baratron gauge is used to measure the pressure in the cell in the range $10^{-2}-10^{5}$ Pa. Before adsorption measurements, self-supported calcined zeolite wafers positioned in the sample holder are first evacuated in the heat chamber under a vacuum of 10^{-2} Pa at 673 K for 12 h. After being cooled at room temperature, the sample is moved down in the optical cell to collect FTIR spectra in the 1725X Perkin-Elmer spectrometer. The sample is then exposed to increasing chloroalkene saturated vapor pressures controlled by the "cold point" technique.[27,35,45]

The amounts adsorbed at constant pressure are determined from the corresponding sorption isotherms obtained by thermogravimetry. Spectra of the cell under air, vacuum, and controlled vapor pressures were used as backgrounds to characterize the sample in the initial, activated, and sorbate loaded states, respectively. Two milligrams of sample was used to analyze a lot of lattice zeolite vibrations without any DTGS detector saturation. Spectra were obtained by co-adding 500 scans to improve the signal-to-noise ratio.

3. Results and Discussion

FTIR Spectra of Pure Chloroalkenes in Gaseous, Liquid, and Solid Phases. PCE and TCE are planar molecules of

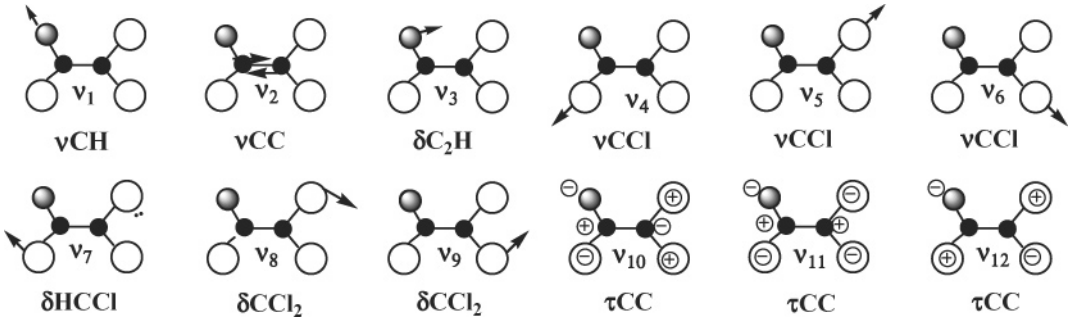

Figure 3. Infrared/Raman active fundamental vibrations[46] of the trichloroethylene molecule. Plus (+) and minus (−) signs are used to represent a torsion movement ahead and behind of the plane of the molecule (●, C; gray ○, H; ○, Cl).

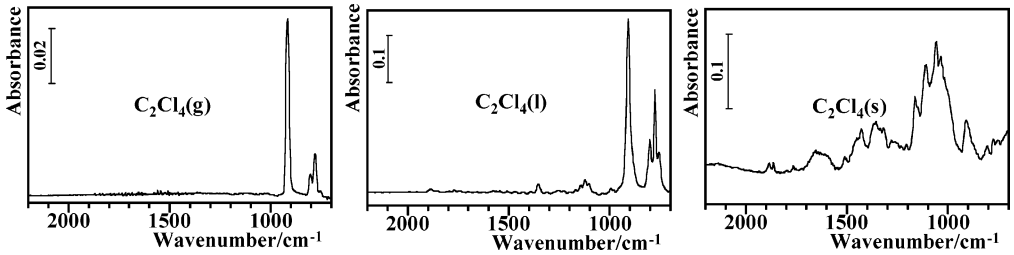

Figure 4. FTIR spectra of tetrachloroethylene in gaseous (g), liquid (l), and solid (s) phases (the broad band located at around 1640 cm^{-1} for C_2Cl_4(s) corresponds to the bending vibration of water).

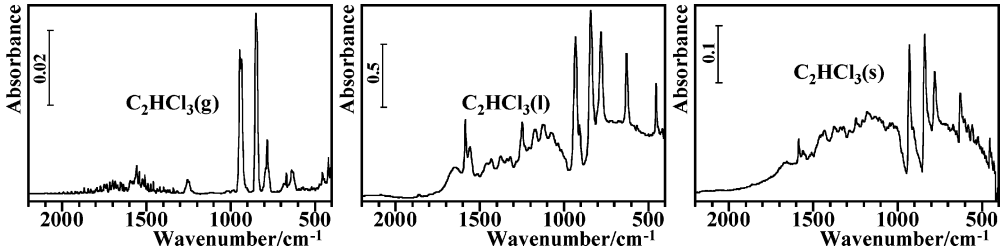

Figure 5. FTIR spectra of trichloroethylene in gaseous (g), liquid (l), and solid (s) phases.

TABLE 1: Location and Assignment of Infrared Vibration Bands of Gaseous, Liquid, and Solid PCE[a]

ν(gas)/cm^{-1}		ν(liquid)/cm^{-1}		ν(solid)/cm^{-1}	
this work	literature[47]	this work	literature[47−52]	this work	assignment
		2482w	2475w, 2470w	2484m	$\nu_1+\nu_9$
		1884w	1887w, 1884w	1884w	$\nu_5+\nu_9$
		1857w	1862w, 1858w	1864w	$\nu_1+\nu_{12}$
		1794w	1795vw	1796w	$\nu_1+\nu_7$
		1770w	1773w, 1771w	1764w	$\nu_5+\nu_{11}$
		1354w	1355m, 1360w	1356m	$\nu_2+\nu_9$
		1255w	1253w, 1254w	1280w	$\nu_6+\nu_9$
		1227w	1222w, 1225w		$\nu_2+\nu_{11}$
			1200w	1206w	$\nu_2+\nu_7+\nu_8$
		1171w	1171w, 1172w	1164s	$\nu_5+\nu_{10}$
		1144w	1142m, 1143w	1109s	$\nu_3+\nu_9$
		1124w	1121m, 1125w	1057vs	$\nu_6+\nu_{11}$
		1104w	1102m, 1102w	1036s	$\nu_6+\nu_7+\nu_8$
		994w	994m, 995w		$\nu_3+\nu_{11}$
		980w	979m, 983w		$\nu_3+\nu_7+\nu_8$
916vs	913vs	910vs	908vvs, 913vs	911m	ν_9
804m	802s	802m	800s, 802s	806m	$\nu_8+\nu_{12}$
781m	782vs	778vs	777vs, 782vs, 792vs	776m	ν_{11}
756w	755m	758m	755s, 758m	754m	$\nu_7+\nu_8$

[a] v, very; w, weak; m, medium; s, strong.

symmetry D_{2h} and C_s, respectively. Five fundamental vibration modes are infrared active for PCE (Figure 2). Twelve fundamental vibration modes are all active in both Raman and infrared for TCE[46−48] (Figure 3).

Figures 4 and 5 show the experimental infrared spectra of PCE and TCE, respectively, in gaseous, liquid, and solid phases. The assignment of vibration bands is given in Tables 1 and 2. Our experimental data are in good agreement with published data.[47−53] The position of fundamental vibration bands of PCE and TCE depends on the physical state of the chloroalkene. A red shift of around 5 cm^{-1} of the $\nu_{11}(\nu_s CCl)$ and $\nu_9(\nu_{as} CCl)$ PCE vibration bands is observed when the state of the chloroalkene changes from a gas to a solid via a liquid and from a gas to a liquid via a solid, respectively. A red shift of

TABLE 2: Location and Assignment of Infrared Vibration Bands of Gaseous, Liquid, and Solid TCE[a]

ν(gas)/cm^{-1}		ν(liquid)/cm^{-1}		ν(solid)/cm^{-1}	
this work	literature[46,53]	this work	literature[46,54]	this work	assignment
3100w	3095m, 3079s	3084m	3080m	3082m	ν_1
	1590m, 1590s	1586s	1585m	1586m	ν_2*
1558w	1555m	1560m	1555w	1558w	ν_2*
1252w	1250m, 1250s	1248m	1248s	1246w	ν_3
941vs	940s, 933s	931s	933s	930s	ν_4
905vs	904w	908s	907m	907w	$2\nu_{11}$
850vs	850s, 850s	842s	842s	838s	ν_5
784m	784s, 783s	781s	783s	780s	ν_{10}
633w	633s, 630s	629s	630s	628m	ν_6
456w	452s	454s	452s	451m	ν_{11}

[a] v, very; w, weak; m, medium; s, strong; *, resonance doublet.

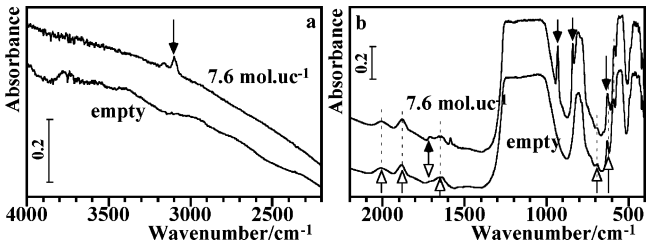

Figure 6. In situ FTIR spectra of ZSM-5 (Si/Al = 500) recorded at room temperature for the activated (empty) material and for an amount of trichloroethylene adsorbed of 7.6 molec.uc^{-1}. The closed and open arrows point the analyzed bands for the adsorbate and the adsorbent, respectively. The double arrow indicates the position of one emerging band.

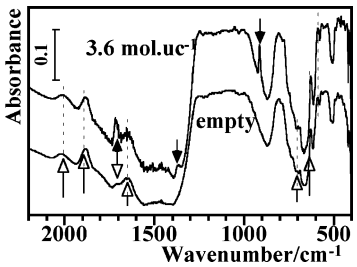

Figure 7. In situ FTIR spectra of ZSM-5 (Si/Al = 500) recorded at room temperature for the activated (empty) material and for an amount of tetrachloroethylene adsorbed of 3.6 molec.uc^{-1}. The closed and open arrows point the analyzed bands for the adsorbate and the adsorbent, respectively. The double arrow indicates the position of one emerging band.

the same order of magnitude is also observed for the $\nu_3(\delta C_2H)$, $\nu_6(\nu CCl)$, $\nu_{11}(\tau CC)$, and $\nu_{10}(\tau CC)$ vibration bands of TCE when the state of the chloroalkene changes from a gas to a solid via a liquid. This red shift is increased up to 12 cm^{-1} for $\nu_5(\nu CCl)$ and $\nu_4(\nu CCl)$ and to 18 cm^{-1} for $\nu_1(\nu CH)$.

In the following section, the position of fundamental vibration bands of the chloroalkenes in gaseous, liquid, and solid phases is used as a reference to characterize the state of the phase adsorbed in the zeolite.

In Situ FTIR Study of the Adsorption of Chloroalkenes on ZSM-5. Before we present the experimental results, some comments should be mentioned. At first, the infrared measurements were performed on a self-supported zeolite showing physical properties close to those of the parent powder zeolite. Therefore, the data obtained by FTIR spectroscopy or by other previously used experimental techniques can be compared without misinterpretation. Second, the infrared spectra were collected under pure saturated vapor pressure at increasing sorbate loadings at room temperature. The amounts adsorbed at the equilibrium were determined from the corresponding sorption isotherms obtained by thermogravimetry. Third and last, for sake of clearness, the experimental results are discussed in the following sections, considering successively the modifications in shape, location, and area of vibration bands of the adsorbate, those of the adsorbent, and then those of an emerging band. The area of vibration bands expressed in cm^{-1} is determined using the Perkin-Elmer Spectrum v2.00 software, with a statistical uncertainty of around 8%. For a given vibration band, the integration was performed using a baseline, a straight line that connects the wavenumber limits defined in Figures 8, 11, 14c,d, 15c,d, 16c−f, 17 and the peak envelop. Figures 6 and 7 show, for example, how the spectrum of the zeolite is changed with a TCE and PCE loading of 7.6 and 3.6 molec.uc^{-1}, respectively. The spectrum of the zeolite, which is not significantly modified in the wavenumber domain 4000−2200 cm^{-1} for PCE adsorption, is not shown in Figure 7.

Physical State of the Adsorbed Phase. Figure 8 shows the evolution of the $\nu_1(\nu CH)$, $\nu_2(\nu CC)$, $\nu_4(\nu CCl)$, and $\nu_5(\nu CCl)$ fundamental vibration bands of TCE with respect to the amount adsorbed in the zeolite. The assignment of these bands is unambiguous because the empty zeolite exhibits no vibration band at the corresponding wavenumbers. These vibration bands appear as soon as the first amount (4.4 molec.uc^{-1}) of TCE is adsorbed (Figure 8). The location dependence curves are shown in Figure 9. Horizontal lines indicate the location of the corresponding fundamental vibration bands for the TCE molecules in the gaseous, liquid, and solid phases. The state of the adsorbed phase slightly changes within a wide domain of micropore filling (n > 4.4 molec.uc^{-1}). The adsorbed phase may be seen as a condensed phase. The TCE molecules, which are mainly confined in micropores, are disposed of one another in such a way that (i) the $\nu_2(\nu CC)$, $\nu_4(\nu CCl)$, and $\nu_5(\nu CCl)$ bonds vibrate at frequencies close to those for molecules in a condensed phase (Figure 9b−d), and (ii) the $\nu_1(\nu CH)$ vibration bond vibrates at a frequency close to the one for molecules in gaseous phase (Figure 9a). The location dependence curve for the $\nu_1(\nu CH)$ vibration band gives some information about the adsorption process of TCE molecules with ZSM-5. At first, at low loading (4.4 molec.uc^{-1}), hydrogen atoms of isolated polar molecules may be suspected to preferentially interact with the oxygen atoms of the zeolite, because the $\nu_1(\nu CH)$ vibration band is red shifted by around 7 cm^{-1} with respect to the one for the molecules in the gaseous phase. Next, on increasing loading above 6 molec.uc^{-1}, adsorbate/adsorbate interactions prevail over adsorbent/adsorbate interactions, as stated by previous calorimetric studies. TCE molecules no more preferentially interact with the oxygen atoms of the zeolite via their hydrogen atoms, but one another. In that case, polar molecules may be disposed end-to-end, allowing the CH bond, the smallest bond of the molecule, to vibrate at a frequency close to the one for the molecules in the gaseous phase.

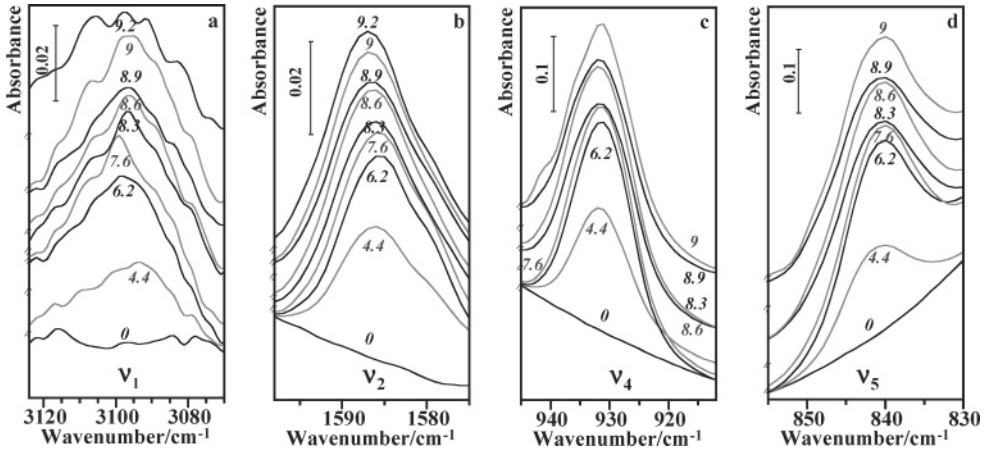

Figure 8. In situ FTIR spectra of the $\nu_1(\nu\text{CH})$ (a), $\nu_2(\nu\text{CC})$ (b), $\nu_4(\nu\text{CCl})$ (c), and $\nu_5(\nu\text{CCl})$ (d) fundamental vibration bands of trichloroethylene adsorbed in ZSM-5 at room temperature. The number of molecules adsorbed per unit cell is given in italic.

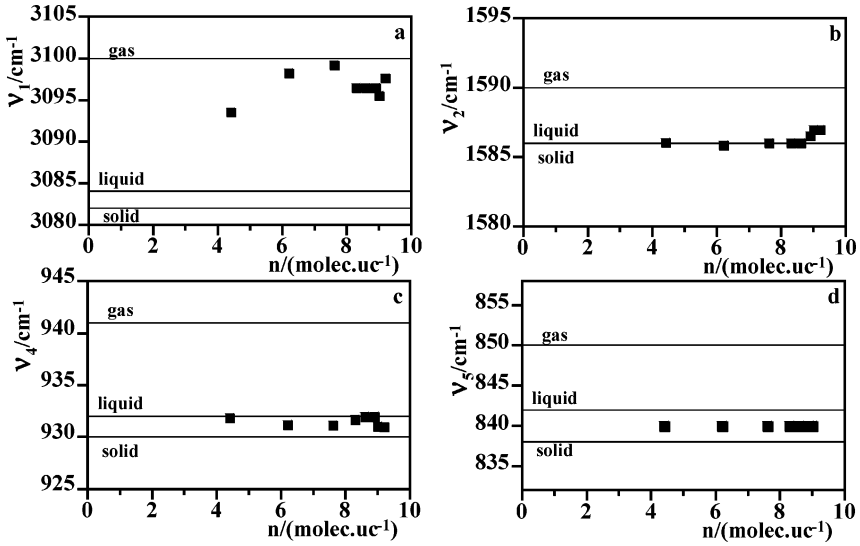

Figure 9. Dependence of the location of the $\nu_1(\nu\text{CH})$ (a), $\nu_2(\nu\text{CC})$ (b), $\nu_4(\nu\text{CCl})$ (c), and $\nu_5(\nu\text{CCl})$ (d) fundamental vibration bands of trichloroethylene adsorbed in ZSM-5, on micropore loading. Horizontal lines define the location of the corresponding vibration bands for trichloroethylene in gaseous, liquid, and solid phases.

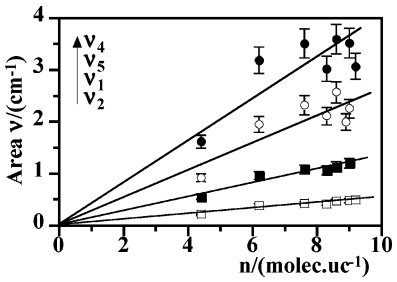

Figure 10. Dependence of the area of the $\nu_1(\nu\text{CH})$ (■), $\nu_2(\nu\text{CC})$ (□), $\nu_4(\nu\text{CCl})$ (●), and $\nu_5(\nu\text{CCl})$ (○) fundamental vibration bands of trichloroethylene adsorbed in ZSM-5, on micropore loading.

As expected, the area everyone investigated of vibration bands linearly increases with loading, within uncertainty limits (Figure 10). This means that the area of vibration bands per molecule adsorbed is quite constant during the adsorption process and, thereby, the environment of TCE molecules does not significantly change upon loading. This result may be compared with the adsorption mechanism of TCE molecules elucidated by Floquet et al.:[30] the micropore filling proceeds by sites, but the TCE molecules are randomly distributed on the three adsorption sites I, II, and III (Figure 1).

For PCE adsorption, two vibration bands may be assigned to the adsorbed phase: the $\nu_9(\nu_{as}\text{CCl})$ fundamental vibration band and the $\nu_2(\nu\text{CC})+\nu_9(\nu_{as}\text{CCl})$ combination band. Figure 11 shows the dependence of the shape of these bands on loading. The state of the adsorbed phase was characterized from the location of the strongest $\nu_9(\nu_{as}\text{CCl})$ vibration band of PCE in

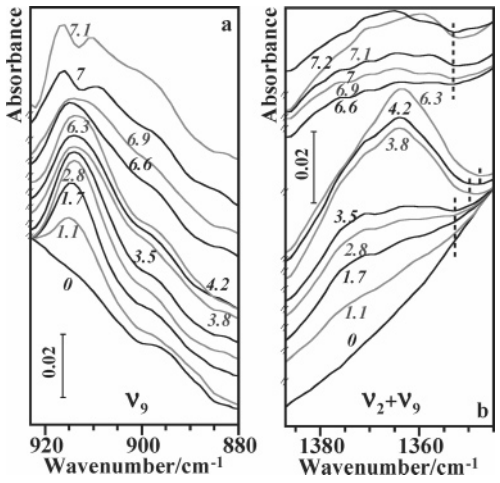

Figure 11. In situ FTIR spectra of the $\nu_9(\nu_{as}\text{CCl})$ (a) and $[\nu_2(\nu\text{CC})+\nu_9(\nu_{as}\text{CCl})]$ (b) vibration bands of tetrachloroethylene adsorbed in ZSM-5 at room temperature. Vertical dashed lines in (b) define the right limits of integrated domains for the determination of band areas.

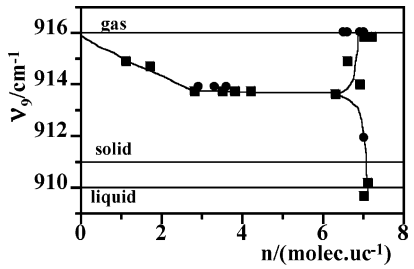

Figure 12. Dependence of the location of the $\nu_9(\nu_{as}CCl)$ vibration band of tetrachloroethylene in ZSM-5, on micropore loading. Horizontal lines define the location of the $\nu_9(\nu_{as}CCl)$ vibration band for tetrachloroethylene in gaseous, liquid, and solid phases. Square and circle symbols are used to differentiate two series of experiments.

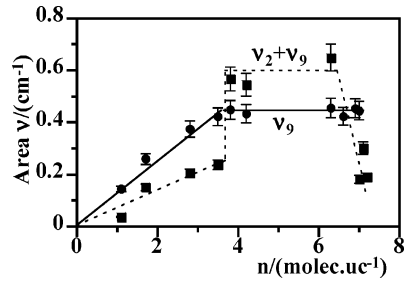

Figure 13. Dependence of the area of the $\nu_9(\nu_{as}CCl)$ (●) and $[\nu_2(\nu CC)+\nu_9(\nu_{as}CCl)]$ (■) vibration bands of tetrachloroethylene adsorbed in ZSM-5, on micropore loading.

gaseous, liquid, and solid phases (Figure 12). Three domains of micropore loading are evidenced. Below around 3 molec.uc^{-1}, the adsorbed phase is close to a phase between a gas and a solid. Between 3 and 6.5 molec.uc^{-1}, the state of the adsorbed phase no more changes with loading and is close to a solid phase. The $\nu_9(\nu_{as}CCl)$ vibration band is then split on approaching micropore saturation. This splitting may be due to the formation of two phases, a liquid and a gas. On this assumption, the liquid phase would result from the condensation of molecules in micropores and the gaseous phase from an accumulation of gaseous molecules on the external surface of the zeolite. On the other hand, the area of this vibration band first linearly increases with loading up to around 4 molec.uc^{-1}, where a step is observed in the isotherm at 298 K, and then stays quite constant on increasing further loading (Figure 13). The first part of the area curve suggests that the environment of the first four adsorbed molecules is not modified. This assumption is supported by previous studies again, showing that the molecules are only located at the intersections of straight and sinusoidal channels (sites III).[30] The horizontal part of the area curve is curious because it does not account for the presence of additional molecules. It may be the consequence of the formation of PCE dimers, the four additional molecules being located in either straight or sinusoidal channels.[30] This assumption supposes that the vibration band of the four external CCl bonds of the dimer is the same in area and location, as the $\nu_9(\nu_{as}CCl)$ vibration of isolated PCE molecules. Moreover, it could be suspected the emergence of at least one additional shifted band due to the contribution of the "internal" CCl bonds of the dimer. The $\nu_2(\nu CC)+\nu_9(\nu_{as}CCl)$ combination band was not characterized in location because this band shows a broad maximum. The corresponding area curve displays a particular shape again, which depends on micropore loading (Figure 13). At first and as expected, the area linearly increases with loading below around 4 molec.uc^{-1}. It then steeply increases at 4 molec.uc^{-1} and stays quite constant up to around 6.5 molec.uc^{-1}, before linearly decreasing on approaching micropore saturation. At this time, we are not able to explain the evolution of the area of this combination band from half loading. Nevertheless, the presence of a "step" in the area curve points out a singularity in the mechanism of PCE adsorption at 4 molec.uc^{-1} again.

Evolution of Zeolite Vibration Bands. Zeolite framework vibrations give rise to typical bands in the mid- and far-infrared. A distinction is currently made between external and internal vibrations of tetrahedra. The original assignments[55−58] of the main infrared bands were as follows:

(i) internal tetrahedra: 1250−920 cm^{-1}, asymmetric stretching; 720−650 cm^{-1}, symmetric stretching; 500−420 cm^{-1}, T−O bending;

(ii) external linkages: 650−500 cm^{-1}, double ring vibrations; 420−300 cm^{-1}, pore opening vibrations; 1150−1050 cm^{-1}, asymmetric stretching; 820−750 cm^{-1}, symmetric stretching.

More recent detailed analysis, however, showed that these assignments have to be revised in some respect. Computation of normal modes suggested that the concept of strictly separated external and internal tetrahedral vibrations must be modified in that zeolite framework vibrations appear to be strongly coupled. Smirnov and Bougeard[59−61] pointed out the necessity to take into account the size of the secondary building units O−T−O and T−O−T for the assignment of FTIR vibration bands.[60−62] The fundamental modes of vibration of small secondary building units of type O−T−O or T−O−T are not located in a narrow wavenumber range but cover a wide domain over more than 100 cm^{-1}. For instance, the spectrum of the symmetric stretching vibration known as ν_s(T−O−T) in the literature[55−58] is not defined by a single band at 800 cm^{-1} but by a main band located at around this position and secondary bands over the wavenumber range 800−100 cm^{-1}. Another example may be given for the angle bending δ(T−O), which gives a discontinuous absorption over 600−50 cm^{-1} and a main band at around 450 cm^{-1}. For these two examples, the main contributions at 800 and 450 cm^{-1} are, for practical reasons, still assigned[55−58] to ν_s(T−O−T) and δ(T−O), respectively. Such a trend may be generalized to practically all vibration modes of small secondary units, except for asymmetric stretching (ν_{as}) vibrations, which are characterized in narrow absorption domains ranging from 1200 to 1000 cm^{-1}. The larger structural building units, such as double rings and pore openings, do not show apparently specific vibration modes, and, therefore, their initial assignment to vibration bands over the wavenumber range 650−500 cm^{-1} is questionable. Thereafter, we will present here only a descriptive analysis of the FTIR spectra of the zeolite.

Four zeolite vibration bands were analyzed to account for the adsorption process within a wide domain of micropore loading. Two of them are complex bands of zeolite framework located at around 689 and 628 cm^{-1} at zero loading. According to the original nomenclature, these bands are assigned to symmetric stretching and double ring vibrations of external tetrahedra, respectively. The two other bands located at around 1883 and 2012 cm^{-1} at zero loading are assigned to overtones of asymmetric stretching vibrations of internal tetrahedra.

As for the characterization of the adsorbed phase, zeolite vibration bands were analyzed in shape, area, and location as a function of loading (Figures 14−16). The presence of admolecules induces a decrease of the area of zeolite vibration bands over a wide domain of micropore loading and therefore, as suspected, hinders zeolite vibrations, except for the vibration located at 628 cm^{-1} for TCE adsorption (Figures 14a, 15a, 16a,b). Moreover, the decrease in area at constant loading is higher (or at least equal) for PCE adsorption than for TCE adsorption. It should be pointed out that in the case of PCE

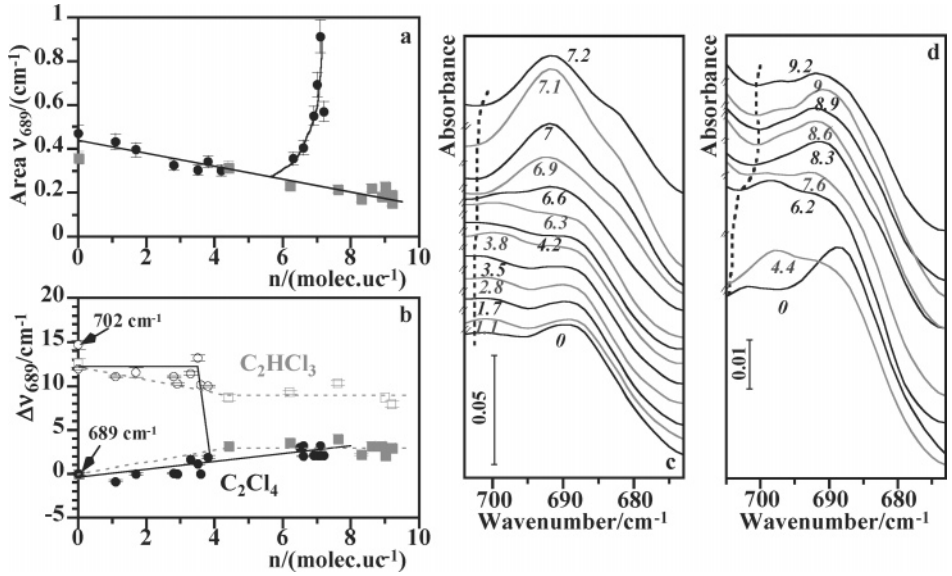

Figure 14. Variation of the area (a), location (b), and shape (c, d) of the complex zeolite vibration band located at around 689 cm^{-1} at zero loading, during the adsorption of tetrachloroethylene (●, ○, c) and trichloroethylene (■, □, d) on ZSM-5. Vertical dashed lines in (c) and (d) define the left integration limits for the determination of band areas. Closed and open symbols in (b) are used to differentiate the main band and the shoulder of the complex band, respectively. The number of adsorbed molecules per unit cell in (c) and (d) is given in italic.

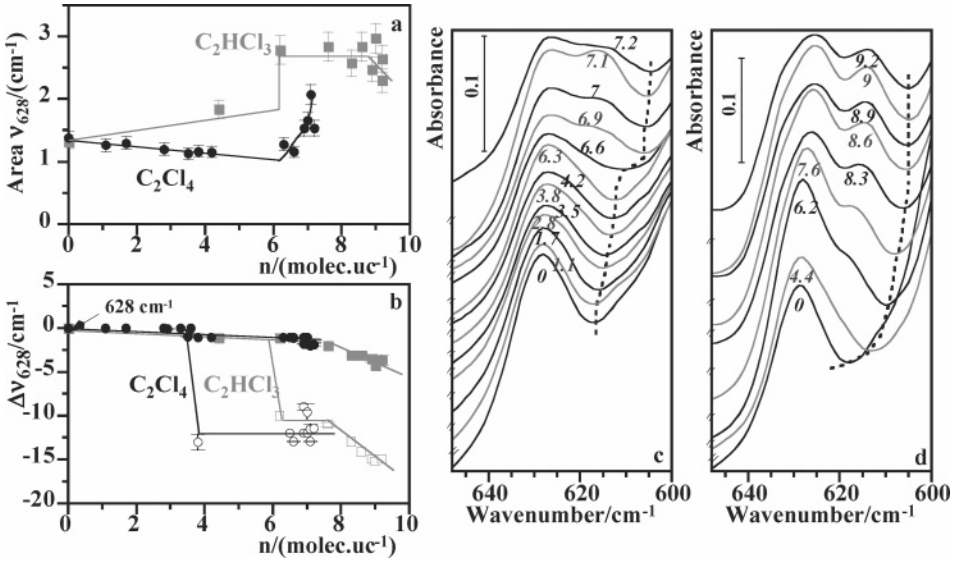

Figure 15. Variation of the area (a), location (b), and shape (c, d) of the complex zeolite vibration band located at around 628 cm^{-1} at zero loading, during the adsorption of tetrachloroethylene (●, ○, c) and trichloroethylene (■, □, d) on ZSM-5. Vertical dashed lines in (c) and (d) define the right integration limits for the determination of band areas. Closed and open symbols in (b) are used to differentiate the main band and the emerging shoulder of the complex band, respectively. The number of adsorbed molecules per unit cell in (c) and (d) is given in italic.

adsorption, the area curves for overtones show a plateau region between 4 and 6.5 molec.uc^{-1}, where a stepwise increase[27] of the amount adsorbed is observed in the isotherm at 298 K. This difference in behavior between PCE and TCE may be correlated with previous microscopic studies, indicating that PCE molecules are more localized than TCE molecules.[30]

However, the complex band located at 628 cm^{-1} (Figures 15a,d) appears to be exacerbated by the presence of TCE molecules. It may be the consequence of an additional contribution of the $\nu_6(\nu CCl)$ vibration band, which should be present at around 630 cm^{-1}, and/or the fact that the complex band significantly changes in shape and becomes broader and broader on increasing loading. This last consideration may also explain why the area of the two complex zeolite bands is increased at high PCE loading (Figures 14a, 15a).

From a general point of view, area curves display particular loadings already identified by previous thermodynamic and structural studies,[26,29,30,35] at around 4 and 6.5 molec.uc^{-1} for PCE adsorption and at around 6 molec.uc^{-1} for TCE adsorption.

Otherwise, vibration bands were characterized in location, except overtones, which show a broad maximum. Figure 14b shows the evolution of one complex vibration band, which consists of a main band and a shoulder located at 689 and 702 cm^{-1} at zero loading, respectively. The main band is continuously blue shifted with increasing loading for both adsorbates. The shoulder is first red shifted up to 4 molec.uc^{-1} and then does not change in location upon loading for TCE adsorption while it stays at the same position up to 4 molec.uc^{-1} before disappearing above this loading for PCE adsorption. For comparison, the second complex band located at 628 cm^{-1} at zero loading is continuously red shifted with loading for both adsorbates (Figure 15b). In that case, the presence of admolecules induces a shoulder at 616 cm^{-1}, which appears at 4 and 6 molec.uc^{-1} for PCE and TCE adsorption, respectively.

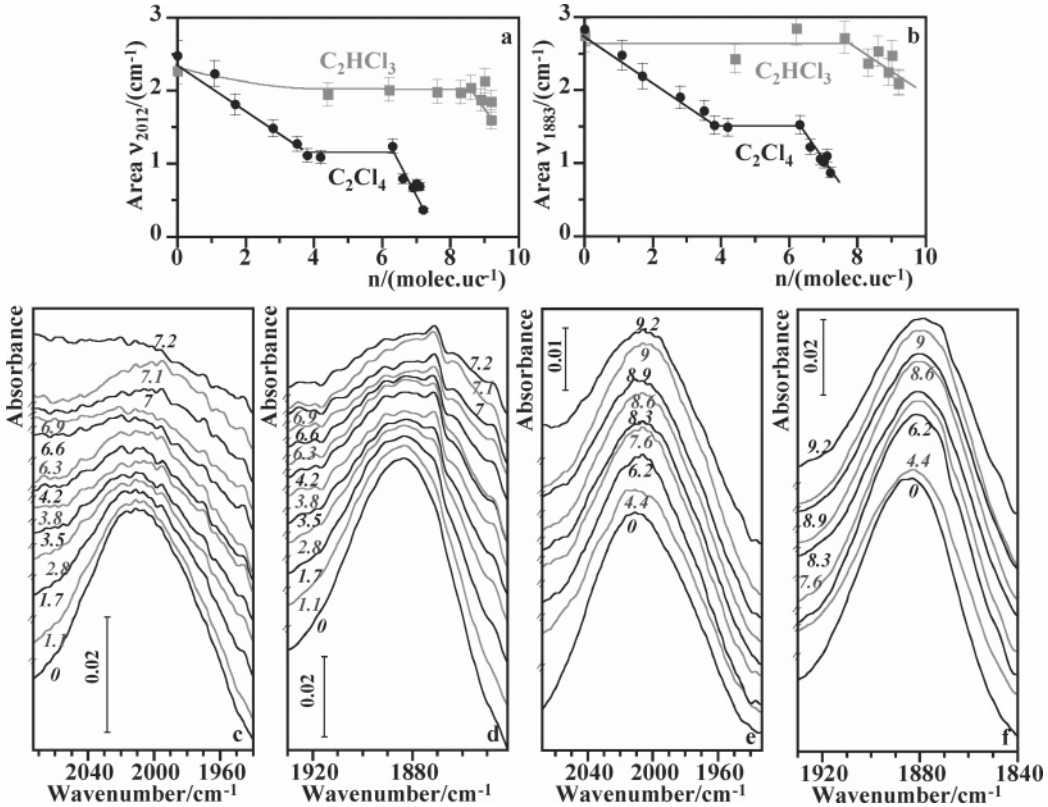

Figure 16. Variation of the area (a, b) and shape (c−f) of zeolite overtones located at around 2012 and 1883 cm^{-1} at zero loading, during the adsorption of tetrachloroethylene (●, c, d) and trichloroethylene (■, e, f) on ZSM-5. The number of adsorbed molecules per unit cell in (c) and (d) is given in italic.

Therefore, for the two investigated complex bands, the adsorption process induces a weak modification of the adsorbent with both adsorbates because the shift of vibration bands is at the most around 3 cm^{-1}. Although this shift is of the same order as the spectral resolution (4 cm^{-1}), this value is considered as significant because of the reproducibility of the experiments from zero loading up to micropore saturation.

Characterization of an Emerging Vibration Band. The infrared spectra of ZSM-5 recorded at increasing loading show in addition to characteristic sorbate and zeolite vibration bands, at least one emerging vibration band located at around 1715 cm^{-1} (Figures 6b, 7, 17). This induced band focused our attention because we also observed it at around the same position for the adsorption of *p*-xylene (*p*-XYL), ethylene (ETH), dichloromethane (DCM), and tetramethylethylene (TME) on the same zeolite.[63−65] Moreover, this band was also reported in the literature[66] for the adsorption of succinic acid on silicalite and assigned to a carbonyl stretching vibration. Such an assignment is now questionable because (i) PCE, TCE, *p*-XYL, ETH, DCM, TME molecules have no carbonyl group and (ii) the emerging band always appears at around the same position, whatever the adsorbate is.

Otherwise, the variation of the area of this band upon loading depends on the nature of the adsorbate and may be seen as a specificity of the type of isotherm (Figure 18). Indeed, in the case of type I isotherms, that is, for the adsorption of TCE or that of DCM, ETH, and TME, the accumulation of molecules induces a continuous increase of the area of the emerging band. In return, in the case of stepped isotherms, that is, for the adsorption of PCE or *p*-XYL, this band increases in area at first continuously then steeply at 4 molec.uc^{-1}, stays quite constant up to around 6.5 molec.uc^{-1}, and finally decreases on increasing further loading.

The emerging band consists of a main band and at least three shoulders located at 1718, 1714, 1708, and 1703 cm^{-1}. It may be assigned to zeolite surface vibrations induced by the presence of admolecules. This assumption is supported by additional in situ infrared measurements performed for PCE adsorption on a nonporous aerosil (Figure 19). The adsorption process also induces an emerging composite band, whose main peak is located at around 1702 cm^{-1}. In that case, we can assume that the main band only accounts for the contribution of the external surface of the nonporous material. By extrapolation with experimental data obtained for TCE and PCE adsorption on ZSM-5, the shoulder located at 1703 cm^{-1} should be representative of the external surface of the adsorbent. Moreover, at the beginning of the adsorption process, the relative intensity of this shoulder is higher for TCE than for PCE, suggesting that the two chloroalkenes do not interact in the same way with the external surface of the zeolite. The amount adsorbed on the external surface would be higher for TCE than for PCE. On the assumption that the shoulder at 1703 cm^{-1} gives a contribution of the external surface of the adsorbent, the main peak and the two other shoulders of the emerging band located at 1718, 1714, and 1708 cm^{-1} would be the contribution of the microporous surface of the zeolite. As a consequence, the change in shape of the emerging band with loading should allow one to describe the adsorption process at a molecular scale. As far as we know, and if we keep in mind[30] that PCE molecules fill first only intersections (up to 4 molec.uc^{-1}) and after straight and sinusoidal channels indifferently, the main band, which is located at 1718 cm^{-1} for PCE adsorption, should be the contribution of molecules adsorbed in the channel intersections because it continuously increases during the accumulation of the first four molecules. Thereby, the two other vibration bands located at 1714 and 1708 cm^{-1} should be representative of the

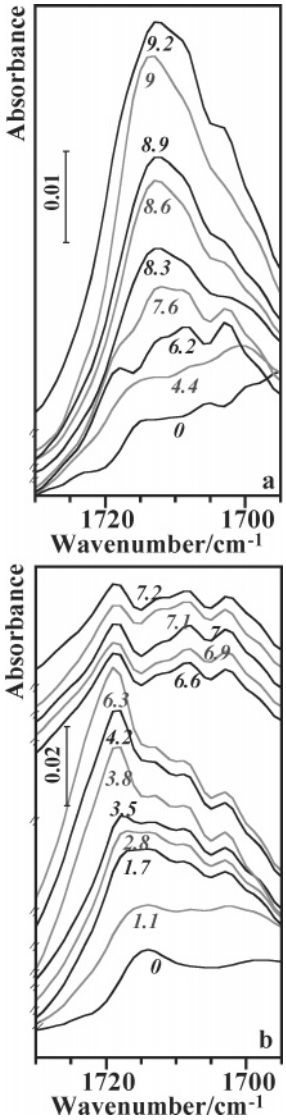

Figure 17. In situ FTIR spectra of one emerging vibration band during the adsorption of trichloroethylene (a) and tetrachloroethylene (b) on ZSM-5 at room temperature. The number of molecules adsorbed per unit cell is given in italic.

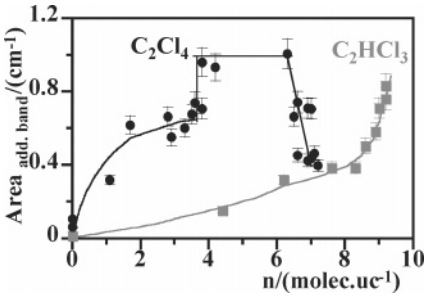

Figure 18. Variation of the area of the emerging band as a function of loading, for the adsorption of tetrachloroethylene (●) and trichloroethylene (■) on ZSM-5 at room temperature.

presence of admolecules in the straight and sinusoidal channels, which cannot be spectroscopically differentiated.

4. Conclusion

This paper reports an infrared spectroscopic study of the interaction of TCE and PCE on a self-supported ZSM-5 zeolite. A systematic study of the evolution of the infrared spectrum of the adsorbent was performed as a function of loading and the nature of the adsorbed phase. All well-defined vibration bands were analyzed in shape, area, and location. Additional experiments were also carried out to characterize the chloroalkenes in solid, liquid, and gaseous phases and thereby the state of the adsorbed phase upon loading. The originality of this work lies in the consideration of both the adsorbent and the adsorbate to analyze the adsorption process.

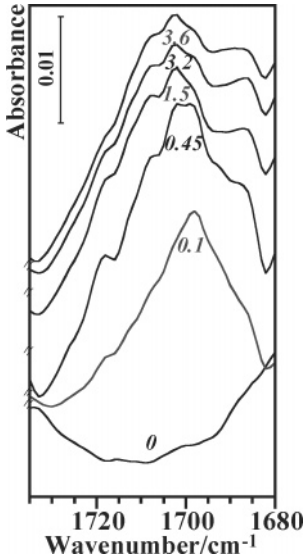

Figure 19. In situ FTIR spectra of a nonporous silica recorded for the adsorption of tetrachloroethylene at increasing saturated pressures. Italic numbers are the pressures in hPa.

The analysis of the $\nu_1(\nu CH)$, $\nu_2(\nu CC)$, $\nu_4(\nu CCl)$, and $\nu_5(\nu CCl)$ vibration bands for TCE accounts for the progressive accumulation of molecules in micropores. As expected, the area of these vibration bands linearly increases with loading over the entire domain of micropore loading. The adsorbed phase may be seen as a condensed phase: the vibrations of $\nu_2(\nu CC)$, $\nu_4(\nu CCl)$, and $\nu_5(\nu CCl)$ bonds are located at frequencies close to those for molecules in a condensed phase, and the vibration of $\nu_1(\nu CH)$ bond is located at a frequency close to that of molecules in gaseous phase. For comparison, the analysis of the $\nu_9(\nu CCl)$ PCE vibration band highlights a singular behavior of the adsorbate. The area of this band linearly increases up to 4 molec.uc^{-1} and then stays quite constant on increasing further loading. The PCE adsorbed phase changes in state from a compressed gas to a phase close to a solid on increasing loading up to around 3 molec.uc^{-1} and then keeps the same state close to a solid up to around 6.5 molec.uc^{-1}. On approaching micropore saturation, two phases, a liquid and a gas, were suspected to be present in micropores and on the external surface of the zeolite.

With regard to the adsorbent, the analysis of four framework vibration bands as a function of loading allowed one to characterize adsorption processes different for PCE than for TCE. The presence of admolecules inhibits zeolite vibration bands, the strongest effects being observed for PCE adsorption. Moreover, the location and area curves account for particular micropore loadings, already highlighted by other experimental approaches. These particular loadings are located at 4 and 6.5 molec.uc^{-1} for PCE adsorption and at 6 molec.uc^{-1} for TCE adsorption.

Another key point of this paper is the characterization of at least one emerging broad vibration band, which gives a fingerprint of the adsorption process. This band is attributed to surface vibrations of the adsorbent modified by the presence of admolecules. It consists of a main band and at least four

shoulders and is located at the same position at around 1715 cm^{-1} for both adsorbates. The analysis of the evolution of this band upon loading, in comparison with spectroscopic data obtained on a nonporous silica, allows one (i) to characterize adsorption processes different for the two chloroalkenes again and (ii) to assign the shoulders at around 1703 cm^{-1} to a vibration of the external surface and the three other components of the broad band at around 1718, 1714, and 1708 cm^{-1} to vibrations of the microporous surface. Moreover, on the basis of the adsorption mechanisms proposed by N. Floquet et al.,[30] we also assumed that the component of the band at 1718 cm^{-1} is representative of the presence of admolecules in the intersections of straight and sinusoidal channels.

References and Notes

(1) Alvarez-Cohen, L.; MacCarty, P. L.; Roberts, P. V. *Environ. Sci. Technol.* **1993**, *27*, 2141.
(2) Cho, I. H.; Kivak, J. H.; Oyoo, R.; Ahn, W. S.; Jung, K. Y.; Park, S. B. *Stud. Surf. Sci. Catal.* **1997**, *105B*, 1617.
(3) Greene, H. L.; Prakash, D. S.; Athota, K. V. *Appl. Catal. B* **1996**, *7*, 213.
(4) Chintawar, P. S.; Greene, H. L. *J. Catal.* **1997**, *165*, 12.
(5) Chintawar, P. S.; Greene, H. L. *J. Appl. Catal. B* **1997**, *14*, 37.
(6) Lopez-Fonseca, R.; Gutierrez-Ortiz, J. I.; Ayastui, J. L.; Gutierrez-Ortiz, M. A.; Gonzalez-Velasco, J. R. *J. Appl. Catal. B* **2003**, *45*, 13.
(7) Schumacher, R.; Ernst, S.; Weitkamp, J. In *Proceedings of the 9th International Zeolite Conference*; Von Ballmoos, R., Higgins, J. B., Treacy, M. M. J., Eds.; Butterworth-Heinemann: Montreal, 1992; p 89.
(8) Niessen, W.; Karge, H. G. *Microporous Mater.* **1993**, *1*, 1.
(9) Thamm, H. *Zeolites* **1987**, *7*, 341.
(10) Guo, C. J.; Talu, O.; Hayhurst, D. T. *AIChE J.* **1989**, *35*, 573.
(11) Lee, C. K.; Chiang, A. S. T. *J. Chem. Soc., Faraday Trans.* **1996**, *92*, 3445.
(12) Song, L. J.; Rees, L. V. C. *Microporous Mesoporous Mater.* **2000**, *35*, 301.
(13) Richards, R. E.; Rees, L. V. C. *Zeolites* **1988**, *8*, 35.
(14) Long, Y.; Sun, Y.; Zeng, H.; Gao, Z.; Wu, T.; Wang, L. *J. Inclusion Phenom. Mol.* **1997**, *28*, 1.
(15) Olson, D. H.; Kokotailo, G. T.; Lawton, S. L. *J. Phys. Chem.* **1985**, *85*, 2238.
(16) Talu, O.; Guo, C. J.; Hayhurst, D. T. *J. Phys. Chem.* **1983**, *93*, 7294.
(17) Richards, R. E.; Rees, L. V. C. *Langmuir* **1987**, *3*, 335.
(18) Vlugt, T. J. H.; Zhu, W.; Kapteijn, F.; Moulijn, J. A.; Smit, B.; Krishna, R. *J. Am. Chem. Soc.* **1998**, *120*, 5599.
(19) Tanaka, H.; Iiyama, T.; Uekawa, N.; Suzuki, T.; Matsumoto, A.; Grün, M.; Unger, K. K.; Kaneko, K. *Chem. Phys. Lett.* **1998**, *293*, 541.
(20) Jänchen, J.; Stach, H.; Busio, M.; Van Wolput, J. H. M. C. *Thermochim. Acta* **1998**, *312*, 33.
(21) Branton, P. J.; Sing, K. W.; White, J. W. *J. Chem. Soc., Faraday Trans.* **1997**, *13*, 2337.
(22) Zhao, X. S.; Ma, Q.; Lu, G. Q. *Energy Fuels* **1998**, *12*, 1051.
(23) Nguyen, C.; Do, D. D. *J. Phys. Chem. B* **2000**, *47*, 11435.
(24) Kokotailo, G. T.; Lawton, S. L.; Olson, D. H.; Meier, W. H. *Nature* **1978**, *272*, 437.
(25) White, J. C.; Hess, A. C. *J. Phys. Chem.* **1993**, *97*, 8703.
(26) Bouvier, F. Thesis, Université de Bourgogne, 1998.
(27) Bouvier, F.; Weber, G. *J. Therm. Anal.* **1998**, *54*, 881.
(28) François, V.; Maure, S.; Bouvier, F.; Weber, G.; Bertrand, O.; Paulin, C. *Stud. Surf. Sci. Catal.* **2001**, *135*, 224.
(29) François, V. Thesis, Université de Bourgogne, 2001.
(30) Floquet, N.; Coulomb, J. P.; Weber, G.; Bertrand, O.; Bellat, J. P. *J. Phys. Chem. B* **2003**, *107*, 685.
(31) Bouvier, F.; Maure, S.; Weber, G.; Bertrand, O. In *Proceedings of the 6th International Conference of Fundamentals of Adsorption*; Meunier, F., Ed.; Elsevier: Paris, 1998; p 171.
(32) Mentzen, B. F.; Lefebvre, F. *Mater. Res. Bull.* **1997**, *22*, 813.
(33) Mentzen, B. F.; Lefebvre, F. *C. R. Acad. Sci. II C* **2000**, *3*, 843.
(34) Mentzen, B. F.; Lefebvre, F. *Mater. Res. Bull.* **2002**, *37*, 957.
(35) Maure, S. Thesis, Université de Bourgogne, 2000.
(36) Zecchina, A.; Scarano, D.; Bordiga, S.; Ricchiardi, G.; Spoto, G.; Geobaldo, F. *Catal. Today* **1996**, *27*, 403.
(37) Busca, G. *Catal. Today* **1998**, *41*, 191.
(38) Jousse, F.; Cohen de Lara, E. *J. Phys. Chem.* **1996**, *100*, 233.
(39) Jousse, F.; Larin, A. V.; Cohen de Lara, E. *J. Phys. Chem.* **1996**, *100*, 238.
(40) Cohen de Lara, E. *Phys. Chem. Chem. Phys.* **1999**, *1*, 501.
(41) Tripathi, A. K.; Sahasrabudhe, A.; Mitra, S.; Mukhopadhyay, R.; Gupta, N. M.; Kartha, V. B. *Phys. Chem. Chem. Phys.* **2001**, *3*, 4449.
(42) Beta, I. A.; Böhlig, H.; Hunger, B. *Phys. Chem. Chem. Phys.* **2004**, *6*, 1975.
(43) Sivasankar, N.; Vasudevan, S. *Catal. Lett.* **2004**, *97*, 53.
(44) Sachsenröder, H.; Brunner, E.; Koch, M.; Pfeifer, H.; Staudte, B. *Microporous Mater.* **1996**, *6*, 341.
(45) Tiselius, A.; Brohult, S. *Z. Phys. Chem.* **1934**, *168*, 248.
(46) Bernstein, H. J. *Can. J. Res. B* **1950**, *2*, 132.
(47) Wu, T. Y. *Vibrational Spectra and Structure of Polyatomic molecules*; Edwards Brothers, Inc.: Ann Arbor, MI, 1946.
(48) Mann, D. E.; Aquista, N.; Plyler, E. K. *J. Res. Natl. Bur. Stand.* **1954**, *52*, 67.
(49) Bernstein, H. J. *J. Chem. Phys.* **1950**, *18*, 478.
(50) Hertzberg, G. *Infrared and Raman Spectra of Polyatomic Molecules*; Van Nostrand, D., Co. Inc.: New York, 1945.
(51) Verleyssen, A. *Ann. Soc. Sci. Brux.* **1939**, 287.
(52) Duchesne, J. *Physica* **1941**, *8*, 144.
(53) Wu, T. Y. *Phys. Rev.* **1934**, *46*, 465.
(54) Allen, G.; Bernstein, G. *Can. J. Chem.* **1954**, *32*, 1044.
(55) Flanigen, E. M. *Adv. Chem. Ser.* **1974**, 80.
(56) Flanigen, E. M.; Bennett, J.; Grose, R. W.; Cohen, J. P.; Patton, R. L.; Kirchner, R. M.; Smith, J. V. *Nature* **1978**, *271*, 512.
(57) Flanigen, E. M.; Khatami, H.; Zymanski, H. A. *Adv. Chem. Ser.* **1971**, *101*, 201.
(58) De Man, A. J. M.; Van Beest, B. W. H.; Leslie, M.; Van Santen, R. A. *J. Phys. Chem.* **1990**, *94*, 2524.
(59) Dumont, D.; Bougeard, D. *Stud. Surf. Sci. Catal.* **1994**, *84*, 2131.
(60) Smirnov, K.; Bougeard, D. *J. Raman Spectrosc.* **1993**, *24*, 255.
(61) Smirnov, K.; Bougeard, D. *Catal. Today* **2001**, *70*, 243.
(62) Zecchina, A.; Bordiga, S.; Spoto, G.; Marchese, L.; Petrini, G.; Leofanti, G.; Padovan, M. *J. Phys. Chem.* **1992**, *96*, 4991.
(63) Bernardet, V.; Decrette, A.; Bertrand, O.; Weber, G.; Simon, J. M.; Bellat, J. P. *Mol. Phys.* **2004**, *102*, 1859.
(64) Bernardet, V.; Decrette, A.; Simon, J. M.; Bertrand, O.; Weber, G.; Bellat, J. P. *Adsorption* **2005**, *11*, 383.
(65) Bernardet, V.; Simon, J. M.; Bertrand, O.; Weber, G.; Bellat, J. P. *Stud. Surf. Sci. Catal.*, in press.
(66) Ikegami, T.; Yanagishita, H.; Kitamoto, D.; Negishi, H.; Haraya, K.; Sano, T. *Desalination* **2002**, *149*, 49.